

## High-energy deuteron measurement with the CAPRICE98 experiment

E. Vannuccini<sup>1</sup>, M. Ambriola<sup>2</sup>, S. Bartalucci<sup>3</sup>, R. Bellotti<sup>2</sup>, D. Bergström<sup>4</sup>, M. Boezio<sup>5</sup>, V. Bonvicini<sup>5</sup>, U. Bravar<sup>6</sup>, F. Cafagna<sup>2</sup>, P. Carlson<sup>4</sup>, M. Casolino<sup>7</sup>, F. Ciacio<sup>2</sup>, M. Circella<sup>2</sup>, C. N. De Marzo<sup>2</sup>, M. P. De Pascale<sup>6</sup>, N. Finetti<sup>1</sup>, T. Francke<sup>4</sup>, P. Hansen<sup>4</sup>, M. Hof<sup>8</sup>, J. Kremer<sup>8</sup>, W. Menn<sup>8</sup>, J. W. Mitchell<sup>9</sup>, E. Mocchiutti<sup>4</sup>, A. Morselli<sup>7</sup>, J. F. Ormes<sup>9</sup>, P. Papini<sup>1</sup>, S. Piccardi<sup>1</sup>, P. Picozza<sup>7</sup>, M. Ricci<sup>3</sup>, P. Schiavon<sup>5</sup>, M. Simon<sup>8</sup>, R. Sparvoli<sup>7</sup>, P. Spillantini<sup>1</sup>, S. A. Stephens<sup>9</sup>, S. J. Stochaj<sup>6</sup>, R. E. Streitmatter<sup>9</sup>, M. Suffert<sup>10</sup>, A. Vacchi<sup>5</sup>, and N. Zampa<sup>5</sup>

<sup>1</sup>University of Firenze and Sezione INFN di Firenze, Florence, Italy

<sup>2</sup>University of Bari and Sezione INFN di Bari, Bari, Italy

<sup>3</sup>INFN – Laboratori Nazionali di Frascati, Frascati, Italy

<sup>4</sup>Royal Institute of Technology, Stockholm, Sweden

<sup>5</sup>University of Trieste and Sezione INFN di Trieste, Trieste, Italy

<sup>6</sup>R. L. Golden Particle Astrophysics Lab, New Mexico State University, Las Cruces, NM, USA

<sup>7</sup>University of Roma “Tor Vergata” and Sezione INFN di Roma II, Rome, Italy

<sup>8</sup>University of Siegen, Siegen, Germany

<sup>9</sup>NASA/Goddard Space Flight Center, Greenbelt, MD, USA

<sup>10</sup>Centre des Recherches Nucléaires, Strasbourg, France

**Abstract.** The CAPRICE98 balloon-borne experiment was flown on 28-29 May 1998 from Fort Sumner, New Mexico, USA. The detector configuration included the NMSU-WiZard/CAPRICE magnetic spectrometer equipped with a gas RICH detector, a silicon-tungsten calorimeter and a time-of-flight system. By combining the RICH and the spectrometer information it was possible to separate <sup>2</sup>H from <sup>1</sup>H in the rigidity range from 29 to 40 GV. We describe the method of analysis and we report results on the <sup>2</sup>H abundance.

### 1 Introduction

The CAPRICE98 balloon-borne experiment (Cosmic AntiParticle Ring Imaging Cherenkov Experiment, 1998) is the latest detector built and flown by the WiZard collaboration. The CAPRICE98 primary science goals were to measure the absolute spectra of positrons and antiprotons along with muon spectra in the atmosphere. Results concerning some of these measurements will be presented during this conference.

The presence of deuterons in cosmic rays is attributed to the interactions of cosmic rays with the interstellar medium during the propagation of the former through the Galaxy. Among other secondary nuclei, deuterons have the advantage of having an interaction mean free path considerably larger than the escape mean free path for cosmic rays from

the Galaxy. For this reason they are a good probe to test propagation models. In spite of its scientific relevance not many measurements exist beyond  $\sim 1$  GeV/n due to the difficult task of identifying deuterons out of the large background of protons.

### 2 The CAPRICE98 apparatus and the flight

The CAPRICE98 apparatus was designed to identify particles in the energy range from few hundreds MeV up to hundreds GeV.

As its basis, CAPRICE98 used the NMSU-WiZard/CAPRICE magnetic spectrometer. This instrument was composed of a drift chamber tracking system ( $\sim 100 \mu\text{m}$  of spatial resolution) (Hof *et al.*, 1994) placed inside the magnetic field generated by a superconducting magnet (0.1 ÷ 2 T inside the tracking volume) (Golden *et al.*, 1978). The tracking system provided 30 position measurements (18 in the bending view and 12 in the non bending one) from which the track deflection ( $\eta$ ) was obtained applying a least-squares fitting procedure (Golden *et al.*, 1991). From the measured deflection we determine the rigidity of the particle ( $R = 1/\eta$ ) and from its sign of the charge. The overall performance of the spectrometer is characterized by the MDR (Maximum Detectable Rigidity) parameter; in the CAPRICE98 configuration the MDR was determined to be  $\sim 300$  GV.

The magnetic spectrometer was surrounded by several sub-detectors whose informations, combined with those of the

spectrometer, enabled particles identification. Starting from the bottom of the payload there were an electromagnetic imaging calorimeter, a TOF (Time-Of-Flight) system and a gas RICH (Ring Imaging Cherenkov) detector.

The CAPRICE98 Si-W electromagnetic calorimeter (total of 7  $X_0$ ) was the same one used for CAPRICE94 and CAPRICE97 (Bocciolini *et al.*, 1996; Ricci *et al.*, 1999). The calorimeter gave both event topology and energy release informations which enabled to distinguish among non interacting particles, electromagnetic showers and hadronic interactions.

The TOF system, which provided both energy loss and timing information ( $\sim 230$  ps of resolution) has been used mainly to reject albedo particles and to perform charge selection.

The RICH detector (Bergstrom *et al.*, 2001) consisted of a photosensitive MWPC, a 1 m tall radiator box filled with high purity  $C_4F_{10}$  gas (refractive index  $n \sim 1.0014$ ) and a spherical mirror. When a particle entered the RICH detector it first traversed the MWPC, then passed through the radiator. If its rigidity was greater than the Cherenkov threshold rigidity ( $R_{th} = (mc/Ze)(\beta\gamma)_{th}$ , where  $(\beta\gamma)_{th} \sim 19$ ) it created a cone of light of width  $\theta_c$  that was reflected back and focused by the spherical mirror toward the MWPC. The upper cathode plane of the MWPC was divided in pads, so that a ring-like image was detected. From the induced signal, combined with the track information coming from the spectrometer, the Cherenkov angle ( $\theta_c$ ) was reconstructed by an iterative procedure. From the measured angle we obtained the particle velocity ( $\beta = n/\cos(\theta_c)$ ) that combined with the measured rigidity enabled particle identification. The RICH detector can also be used as a threshold device.

CAPRICE98 was launched on the 28th of May 1998 from Ft. Sumner, NM, USA ( $34^\circ N$   $104^\circ W$ ). The payload flew for  $\sim 21h$  at a float altitude of  $\sim 5.5$  g/cm $^2$ .

### 3 Data analysis

Using the informations of the TOF system we selected a clean sample of downward going singly-charged events.

Since the tracking information is critical for identifying deuteron, we applied strict selection criteria on the quality of the fitted tracks. The applied cuts required a minimum number of position measurements (11 in the bending direction and 7 in the non bending one), an acceptable  $\chi^2$  for the fitted tracks in both direction and an additional condition on the deflection uncertainty estimated during the fitting procedure ( $\sigma_\eta < 0.008$  GV $^{-1}$ ).

Some geometrical constraints were applied, by requiring the containment of the track inside the tracking volume and the full containment of the Cherenkov ring extrapolated from the tracking information, inside the pad plane. We also rejected multiparticle events using both the top scintillators and the MWPC signals.

The described selection criteria resulted in a sample of well-reconstructed events which contained mainly protons,

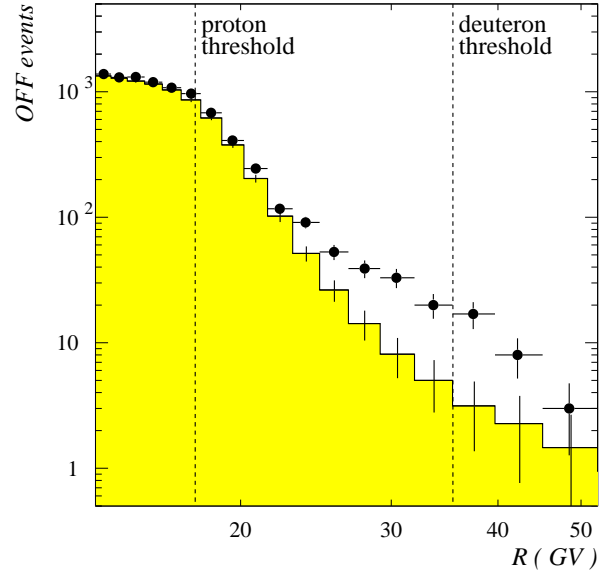


**Fig. 1.** Number of events selected requiring no Cherenkov signal (black circles) and background level obtained from the simulation (shaded area). The threshold rigidity for both protons and deuterons are also shown.

deuterons and a negligible component of muons and mesons.

To select the deuterons we used the RICH detector as a threshold device, requiring that above the proton threshold rigidity (about  $\sim 18$  GV) the event did not produce Cherenkov signal. Fig. 1 (black circles) shows the number of selected events (OFF events) as a function of the rigidity.

The selected sample contains both deuteron and proton events without a Cherenkov signal which represent a non negligible contamination. For this reason its contribution must be estimated and subtracted. Since deuteron identification is possible only using the RICH information the background level was determined using a simulation.

### 4 Instrument simulation

Our approach was to develop an empirical response model of the instrument based on characteristic quantities obtained from experimental data. Using this model it was possible to simulate the instrument response on an event-by-event basis.

The presence of proton events without a Cherenkov signal beyond the threshold is mainly due to the following two effects: 1) the probability of zero detected photoelectrons, that is different from zero even over threshold; 2) the uncertainty in the measured deflection. We need to simulate both these effects in order to estimate the background level.

#### 4.1 The RICH detector response

To simulate the RICH detector response we need the probability of no Cherenkov signal detected ( $P(OFF)$ ) as a function of rigidity. Fig.2 shows the ratio of events without a

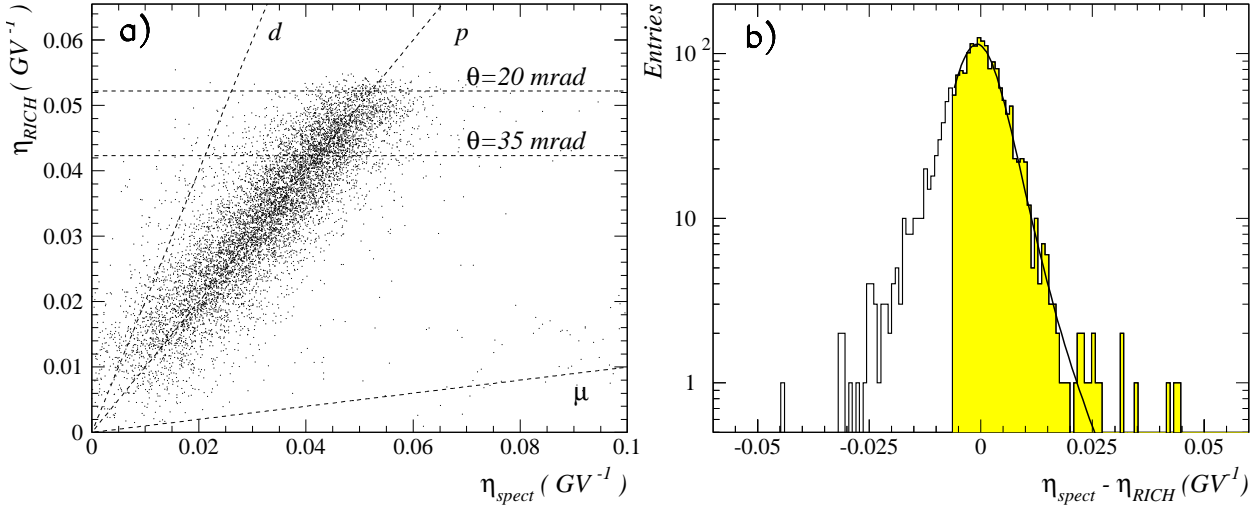


**Fig. 3.** a) Plot of the deflection derived from the reconstructed Cherenkov angle assuming a mass of a proton ( $\eta_{RICH}$ ) as a function of the deflection measured with the spectrometer ( $\eta_{spect}$ ). The inclined dashed lines represent the expected shape for deuterons, protons and muons. The horizontal dashed lines show the applied cuts. b) Distribution of  $\eta_{spect} - \eta_{RICH}$  for the selected sample. The solid line represents a fit to the data (see section 4.2 for more explanation)

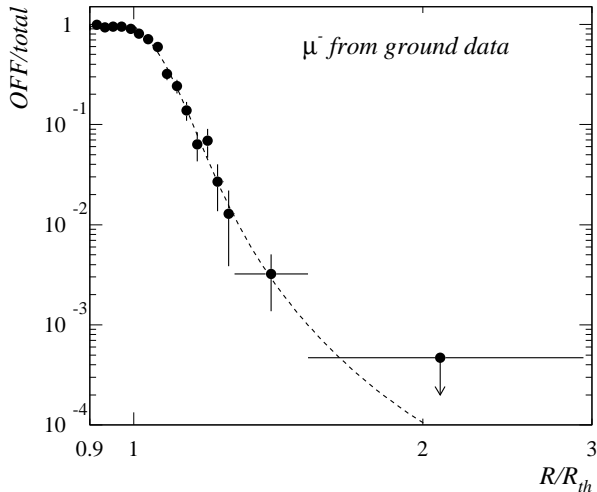


**Fig. 2.** The ratio of OFF events to all events obtained for muons from ground data. The dashed line is a fit to the data.

Cherenkov signal to all events obtained from a large sample of muons from ground data. Since in this rigidity region (the threshold rigidity for muons is  $\sim 2$  GV) the spectrometer uncertainty is negligible, the ratio  $OFF/total$  should give directly  $P(OFF)$ . We plotted this quantity as a function of  $R/R_{th}$  since in terms of this variable it can be scaled to any particle. A non negligible effect could result from low energy muons which measured rigidity is greater than threshold rigidity due to multiple scattering effect; this would lead to an overestimate of  $P(OFF)$ . We anyway took the function obtained from muons as an upper limit for  $P(OFF)$ .

The described procedure is based on the assumption that the RICH detector response was the same at ground and during the flight. This hypothesis has to be verified in order to get reliable results from the simulation. Some preliminary checks have been carry out on flight data and all suggested that the RICH performances didn't change significantly during the flight. Further checks are planned and definitive results will be presented at the conference.

#### 4.2 The spectrometer resolution function

The spectrometer resolution function (SRF) has been obtained using protons from flight data.

We selected a sample of events with rigidity greater than 10 GV and a well-defined ring in the RICH detector; we then derived the deflection ( $\eta_{RICH}$ ) from the reconstructed Cherenkov angle assuming a mass of a proton. In fig.3a this quantity is plotted as a function of the deflection measured with the spectrometer ( $\eta_{spect}$ ). Since the distribution of the variable  $\eta_{spect} - \eta_{RICH}$  is a convolution of the SRF and the resolution function of the RICH detector, by knowing the RICH detector response it is possible to derive the SRF by applying an unfolding procedure. Fig. 3b shows the distribution of  $\eta_{spect} - \eta_{RICH}$  obtained requiring a Cherenkov angle between 20 and 35 mrad; this cut has been applied in order to both minimize the RICH uncertainty and reduce in the sample the contamination of particles different from protons.

To construct the resolution function of the RICH detector the first step was to parameterize the RICH response. As for  $P(OFF)$ , muons from ground data were used. As an example, fig.4 shows the measured angular resolution as a function of  $R/R_{th}$  together with the given parameterization. Using an input power law spectrum in rigidity, proton events in

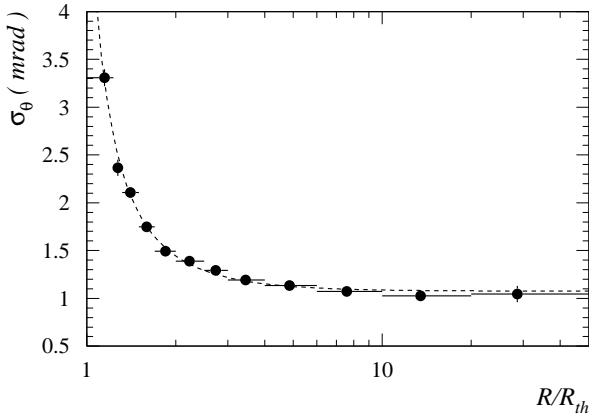


**Fig. 4.** The measured Cherenkov angle resolution obtained for muons from ground data. The dashed line is a fit to the data. The resulting resolution for  $\beta \sim 1$  particles is about 1.1 mrad

the RICH detector was generated, the applied cuts simulated and the RICH resolution function constructed on an event-by-event basis.

To determine the SRF we fitted the distribution shown in fig.3b with a function obtained convolving the RICH resolution function with a Lorentzian which parameters were left free to vary. The solid line in fig.3b represents the results of the fitting procedure; the resulting reduced  $\chi^2$  was  $\sim 0.9$ . To avoid that the deuteron component altered the result the left tail of the distribution was excluded from the fit. We took a Lorentzian with the parameters obtained by the fit as the best estimate of the SRF.

Other procedures exist in literature to derive the SRF from experimental data. Menn *et al.* (2000) derived the SRF making a superposition of Gaussians with width given by the uncertainty on the measured deflection. A second procedure is that one described by Boezio *et al.* (2001), who derived the SRF from magnet-off ground data selecting relativistic muons. Both the obtained SRFs are inadequate to describe the spectrometer response with the required accuracy: the first one because of the assumed gaussian error, the second one because of the non negligible multiple scattering effect. The results of such procedures is the underestimation and the overestimation of the SRF tails, respectively.

#### 4.3 Proton background determination

To determine the shape of the proton background distribution we started with an input power law spectrum in rigidity, with spectral index derived from the all-particles spectrum after the SRF was unfolded. We simulated both proton and deuteron events starting from 5 GV; for each event the RICH signal was generated according to  $P(\text{OFF})$  and the deflection smeared according to the SRF. As a result of the simulation

we obtained both the contamination and the efficiency for deuteron selection as a function of the rigidity.

## 5 Results

In order to determine the number of background events in each rigidity bin we needed to normalize the background events distribution obtained from the simulation.

We considered all the events in the rigidity range  $19 \div 45$  GV and we applied to this sample the deuteron selection criterion. The sample contained both deuterons and background protons. Using the efficiency and contamination values in this rigidity range obtained from the simulation, we estimated the number of background protons and normalized the simulated distribution to that number. The used rigidity range was the one minimizing the relative error on the normalization constant.

The resulting background distribution is shown in fig.1 (shaded area) together with the number of selected events as a function of rigidity. We can see that the proton background dominates the sample up to  $\sim 25$  GV. For increasing rigidity the deuteron component emerges from the background, which reaches its minimum ( $\sim 20\%$  of the selected events) from 29 to 40 GV.

In this range, after background subtraction and selection efficiency correction, the resulting deuteron to proton ratio was  $d/p = (3.9 \pm 0.6)\%$ , at the spectrometer level.

## 6 Conclusions

The highest energy deuterons measurement available is that one of Apparao *et al.* (1973) who gave the deuteron to helium ratio at  $\sim 7.5$  GeV/n ( $\sim 17$  GV for deuteron). At higher energies only an upper limit to the deuteron to helium ratio exists (Golden *et al.*, 1985).

The CAPRICE98 experiment can identify deuterons out of protons in the rigidity range  $29 \div 40$  GV. For the first time it is possible to measure the deuteron flux in this energy domain. Here only preliminary results are given; the final result will be presented at the conference.

## References

- Apparao, K. M. V., et al., Proc. 13th ICRC, 1, 126, 1973
- Bergstrom, D., et al., NIM A, 463, 161, 2001
- Boezio, M., et al., To be published in
- Bocciolini, M., et al., NIM A, 370, 403, 1996
- Menn, W., et al., ApJ, 533, 281, 2000
- Hof, M., et al., NIM A, 345, 561, 1994
- Golden, R. L., et al., Proc. 19th ICRC, 2, 68, 1985
- Golden, R. L., et al., NIM, 148, 179, 1978
- Golden, R. L., et al., NIM A, 306, 366, 1991
- Ricci, M., et al., Proc. 26th ICRC, 5, 49, 1999